Analysis of a Slot Coupled and Stripline Fed Patch Antenna

Jui-Ching Cheng

May 4, 1993

Abstract

A patch antenna that is fed by an open-ended stripline is analyzed. The patch and the stripline are located on different dielectric slabs which are stacked together with a ground plane in between. Coupling is achieved through a slot on the ground plane between the patch and the stripline. The separation of the antenna and feeding structure by the ground plane provides flexibility in design and prevents interference between circuit elements and the antenna.

Full wave analysis and moment method are used in the analysis of this structure. Spectral domain Green's functions of the conductor-backed dielectric slab and two parallel plates waveguide are used in the formulation of the integral equations. Numerical simulation of the input impedance of the antenna with different stub lengths is shown.

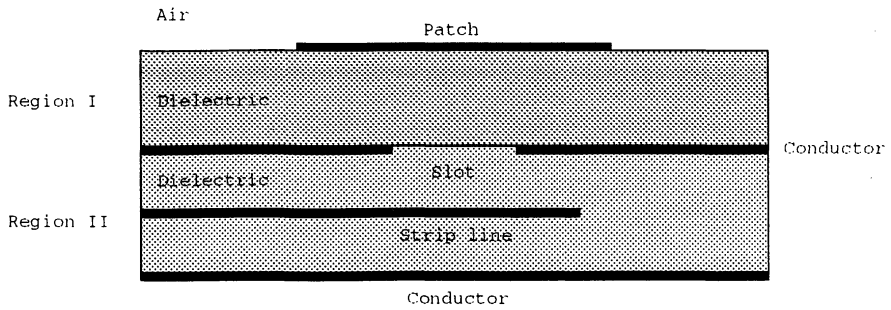

Figure 1: The structure of a slot coupled and stripline fed patch antenna.

1 Introduction

Fig. 1 shows a patch antenna that is fed by an open-ended stripline through a slot opened on the ground plane between the patch and the stripline. Energy is coupled to the patch antenna from the slot. Full wave analysis and moment method are used in the analysis of this structure. Similar structures have been fully analyzed by the same method[1][3][4]. The purpose of this article is not to introduce new method or new structure. It is to establish the computer programs in preparation for another project that combines finite element method and moment method to analyze similar structures.

Section 2 will give a rigorous analysis of the problem. Section 3 shows the numerical results. Pertinent Green's functions are listed in appendix.

2 Theoretical Analysis

The schematic of the antenna and feed line is shown in Fig. 2 with impressed and induced currents indicated. The ground plane and dielectric substrates extend to infinity in the x and y directions. As shown in the figure, $\bar{J}_p$ denotes the induced current on the patch, $\bar{E}_s$ the tangential electric field on the slot, $\bar{J}_{inc}$ the incident traveling current mode on the stripline, and $\bar{J}_f$ the induced current on the stripline due to the field scattered by this structure, including higher order current modes near the open end and the reflected traveling current mode.

By using equivalence principle, the original problem may be changed to

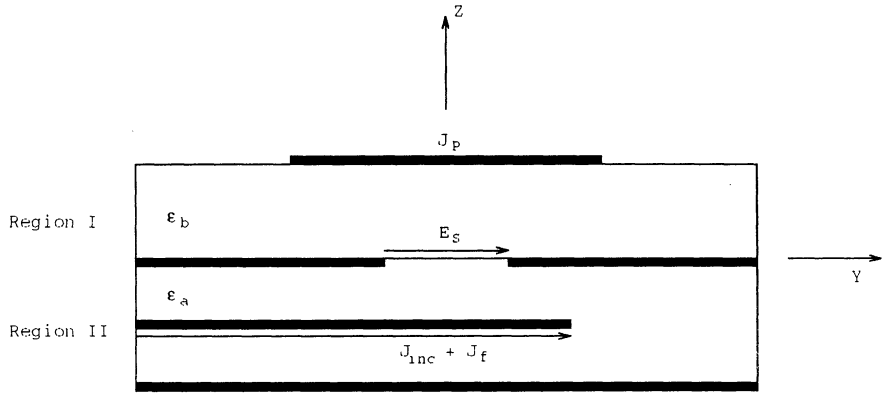

Figure 2: The schematic of the original problem.

an equivalent one which is shown in Fig 3. The slot are closed by conductor such that the original structure is separated to 2 regions. In order to keep the same field distribution as the original one, magnetic surface currents $\bar{M}_s$ must be added on the surface of the slot. Furthermore, $\bar{M}_s$ satisfy

$$\bar{M}_s = \hat{z} \times \bar{E}_s. \tag{1}$$

Let region a denote the lower dielectric slab, region b denote the upper dielectric slab. The total electric and magnetic fields can be represented by superposition of fields due to the various currents as follows:

$$\bar{E}_a^{tot} = \bar{E}_a(\bar{J}_{inc}) + \bar{E}_a(\bar{J}_f) + \bar{E}_a(\bar{M}_s) \tag{2}$$

$$\bar{H}_a^{tot} = \bar{H}_a(\bar{J}_{inc}) + \bar{H}_a(\bar{J}_f) + \bar{H}_a(\bar{M}_s) \tag{3}$$

$$\bar{E}_b^{tot} = \bar{E}_b(\bar{J}_p) - \bar{E}_b(\bar{M}_s) \tag{4}$$

$$\bar{H}_b^{tot} = \bar{H}_b(\bar{J}_p) - \bar{H}_b(\bar{M}_s) \tag{5}$$

Each field in the equation (2)-(5) can be represented by dyadic Green's function for each structure such as

$$\bar{E}_b(\bar{M}_s) = \iint_{slot} \overline{\overline{G}}_{EM}^{b}(x, y, z|x_0, y_0, z_0) \cdot \bar{M}_s \, dx_0 \, dy_0 \tag{6}$$

where $\overline{\overline{G}}_{EM}^{b}$ is the electric field at (x, y, z) due to an infinitesimal magnetic current at (x_0, y_0, z_0) radiating in the presence of a grounded dielectric slab.

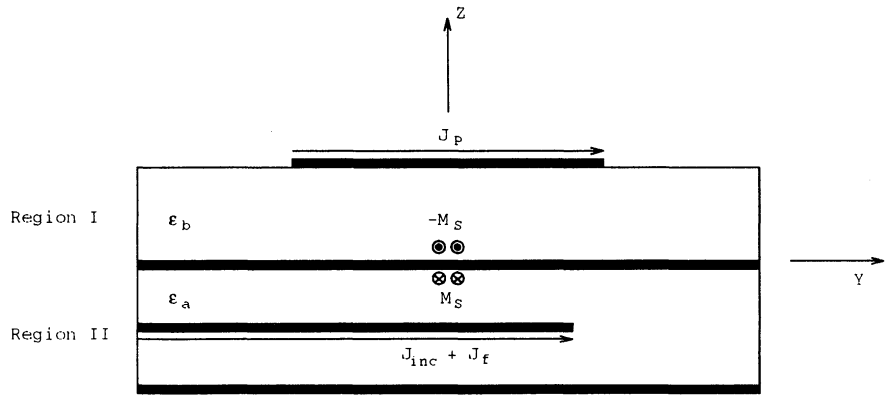

Figure 3: The equivalent problem after closing the slot by conductor. Suitable magnetic currents are added to ensure the equivalence.

This and other Green's functions needed for the analysis are obtained by using spectral domain methods so that

$$\bar{\bar{G}}^b_{EM}(x,y,z|x_0,y_0,z_0) = \int\int_{-\infty}^{\infty} \bar{\bar{Q}}^b_{EM}(k_x,k_y;z,z_0)\cdot e^{jk_x(x-x_0)}e^{jk_y(y-y_0)}\,dk_x\,dk_y \tag{7}$$

Three coupled integral equations are obtained for the three unknown currents $\bar{J}_f$, $\bar{J}_p$, $\bar{M}_s$ by enforcing the boundary conditions: 1) $\bar{E}^{tan} = 0$ on the strip line, 2) $\bar{H}^{tan}$ is continuous through the slot, and 3) $\bar{E}^{tan} = 0$ on the patch. That is

$$\bar{E}_a(\bar{J}_{inc}) + \bar{E}_a(\bar{J}_f) + \bar{E}_a(\bar{M}_s) = 0 \qquad \text{on the stripline} \tag{8}$$

$$\bar{E}_b(\bar{J}_p) - \bar{E}_b(\bar{M}_s) = 0 \qquad \text{on the patch} \tag{9}$$

$$\bar{H}_a(\bar{J}_{inc}) + \bar{H}_a(\bar{J}_f) + \bar{H}_a(\bar{M}_s) = \bar{H}_b(\bar{J}_p) - \bar{H}_b(\bar{M}_s) \qquad \text{on the slot} \tag{10}$$

Galerkin moment method is used to obtain the integral equations linking the unknown currents in region a and b.

The unknown currents are formulated by choosing expansion functions as follows:

$$\bar{J}_p(x,y) = \sum_{n=1}^{N_b} J_n^b \bar{J}_n^b(x,y) \tag{11}$$

$$\bar{M}_s(x,y) = \sum_{n=1}^{N_s} M_n^s \bar{M}_n^s(x,y) \tag{12}$$

$$\bar{J}_f(x,y) = \sum_{n=1}^{N_a} J_n^a \bar{J}_n^a(x,y) + R\bar{J}_{ref}(x,y) \tag{13}$$

Where $\bar{J}_{ref}$ is the reflected traveling current mode on the stripline. Defining an inner product

$$(F,G)_s = \iint_s \bar{F} \cdot \bar{G}\, ds \tag{14}$$

The three boundary conditions lead to

$$-[Z^{inc}] - R[Z^{ref}] - [Z^a][I^a] + [T^a][M^s] = 0 \tag{15}$$

$$[Z^b][I^b] + [T^b][M^s] = 0 \tag{16}$$

$$[C^{inc}] + R[C^{ref}] + [C^a][I^a] - [Y^a][M^s] = [Y^b][M^s] + [C^b][I^b] \tag{17}$$

The matrices and vector elements are defined as follows:

$z^a_{mn} = (-\bar{J}^a_m, \bar{E}_a(\bar{J}^a_n))_f$	$N_a + 1 \times N_a$	matrix	(18)
$y^a_{mn} = (-\bar{M}^s_m, \bar{H}_a(\bar{M}^s_n))_s$	$N_s \times N_s$	matrix	(19)
$t^a_{mn} = (\bar{J}^a_m, \bar{E}_a(\bar{M}^s_n))_f$	$N_a + 1 \times N_s$	matrix	(20)
$c^a_{mn} = (\bar{M}^s_m, \bar{H}_a(\bar{J}^a_n))_s$	$N_s \times N_a$	matrix	(21)
$z^b_{mn} = (-\bar{J}^b_m, \bar{E}_b(\bar{J}^b_n))_p$	$N_b \times N_b$	matrix	(22)
$y^b_{mn} = (-\bar{M}^s_m, \bar{H}_b(\bar{M}^s_n))_s$	$N_s \times N_s$	matrix	(23)
$t^b_{mn} = (\bar{J}^b_m, \bar{E}_b(\bar{M}^s_n))_p$	$N_b \times N_s$	matrix	(24)
$c^b_{mn} = (\bar{M}^s_m, \bar{H}_b(\bar{J}^b_n))_s$	$N_s \times N_a$	matrix	(25)
$c^{inc}_m = (\bar{M}^s_m, \bar{H}_a(\bar{J}_{inc}))_s$	$N_s \times 1$	column vector	(26)
$c^{ref}_m = (\bar{M}^s_m, \bar{H}_a(\bar{J}_{ref}))_s$	$N_s \times 1$	column vector	(27)
$z^{inc}_m = (-\bar{J}^a_m, \bar{E}_a(\bar{J}_{inc}))_f$	$N_a + 1 \times 1$	column vector	(28)
$z^{ref}_m = (-\bar{J}^a_m, \bar{E}_a(\bar{J}_{ref}))_f$	$N_a + 1 \times 1$	column vector	(29)
$I^a_n = J^a_1, J^a_2, \cdots, J^a_{N_a}$	$N_a \times 1$	column vector	(30)
$I^b_n = J^b_1, J^b_2, \cdots, J^b_{N_b}$	$N_b \times 1$	column vector	(31)
$M^s_n = M^s_1, M^s_2, \cdots, M^s_{N_s}$	$N_s \times 1$	column vector	(32)

Note that on the stripline extra higher order current mode is used as a test function to avoid using traveling current mode such that computation

complexity is reduced. From reciprocity it can be seen that the elements of $[T^a]$ are related to $[C^a]$ by

$$t^a_{mn} = -c^a_{nm} \tag{33}$$

Also the elements of $[T^b]$ are related to $[C^b]$ by

$$t^b_{mn} = -c^b_{nm} \tag{34}$$

Recast some of the quantities above into new forms:

$$[Z^a_{tot}] = [z^a_{mn}|z^{ref}_m] \quad N_a + 1 \times N_a + 1 \quad \text{matrix} \tag{35}$$
$$[C^a_{tot}] = [c^a_{mn}|c^{ref}_m] \quad N_s \times N_a + 1 \quad \text{matrix} \tag{36}$$
$$[I^a_{tot}] = [I^a_n|R] \quad N_a + 1 \times 1 \quad \text{column vector} \tag{37}$$
$$[Y_{tot}] = [y^b_{mn} + y^a_{mn}] \quad N_s \times N_s \quad \text{matrix} \tag{38}$$

Substituting the above equations to (15)–(17) and rearranging yields

$$[Z^{inc}] + [Z^a_{tot}][I^a_{tot}] = [T^a][M^s] \tag{39}$$
$$[Z^b][I^b] + [T^b][M^s] = 0 \tag{40}$$
$$[C^{inc}] + [C^a_{tot}][I^a_{tot}] = [Y_{tot}][M^s] + [C^b][Ib] \tag{41}$$

Solving (39)-(41) simultaneously, we get

$$[M^s] = ([C^a_{tot}][Z^a_{tot}]^{-1}[T^a] - [Y_{tot}] + [C^b][Z^b]^{-1}[T^b])^{-1} ([C^a_{tot}][Z^a_{tot}]^{-1}[Z^{inc}] - [C^{inc}]) \tag{42}$$
$$[I^a_{tot}] = [Z^a_{tot}]^{-1}([T^a][M^s] - [Z^{inc}]) \tag{43}$$
$$[I^b] = -[Z^b]^{-1}[T^b][M^s] \tag{44}$$

Such the unknown quantities $[M^s]$, $[I^a_{tot}]$ and $[I^b]$ are solved in terms of matrix equations (42)–(44).

3 Numerical Results

Further simplifications are made to expedite the numerical calculation. Assume the input traveling current is only y directed and without variation along x direction on the stripline. The reflected traveling wave mode and higher order modes on the stripline are also y directed. The slot is assumed

to be very narrow along y direction such that only y component of E field exists on the slot. Since the excitation on the slot is y directed, it is suffice to assume only y directed current exists on the patch. Piecewise sinusoidal current modes(PWS) are used to represent $\bar{J}_p$, $\bar{J}_a$ and $\bar{M}_s$. Only one PWS mode is used to represent $\bar{M}_s$. 5 modes are used for the patch and seven modes for the feedline. Because infinite traveling wave mode introduces additional pole, it is truncated by a sufficient length. In this paper, we choose 3 wavelengths.

Each element of the matrix equation is integrated numerically. The algorithm of integration is 16-point adaptive Gaussian quadrature. The double infinite integration in the k_x, k_y plane is changed to one single infinite integration and one finite integration by converting to polar coordinate[2]. The infinite integration is truncated at $150k_0$. The pole of the stripline structure is removed by pole extraction method[3]. The poles of the patch antenna structure are treated analytically[2].

Fig. 6 to Fig. 9 show the input impedance of the antennas plotted as a function of frequency in Smith chart form. The frequency range is from 2150MHz to 2275MHz with increment of 25MHz. The result of [1] is also plotted together as a comparison. All the parameters are the same for Fig. 6 to Fig. 9 as indicated in Fig. 6 except the stub length. The result is similar to that of [1].

Fig. 10 shows the input impedance of the antenna as a function of stub length at frequency 2220MHz. The locus approximately follows a constant resistance contour. This implies that the aperture and antenna appear as a series load along and open circuited transmission line. This result is the same as [1] as expected.

4 Conclusion

This paper demonstrates the possibility of using spectral domain analysis and moment method in calculating the input impedance of a stipline-feed, slot-coupled patch antenna. Although no experiment data are provided, the result shows good consistency with that of similar structure calculated by the same method. While this is not the purpose of this project, it is to prepare the needed program and analysis to combine with finite element for more complex structures. This will be the next goal for this project.

Appendix

A Derivation of the Spectral Domain Green's Functions

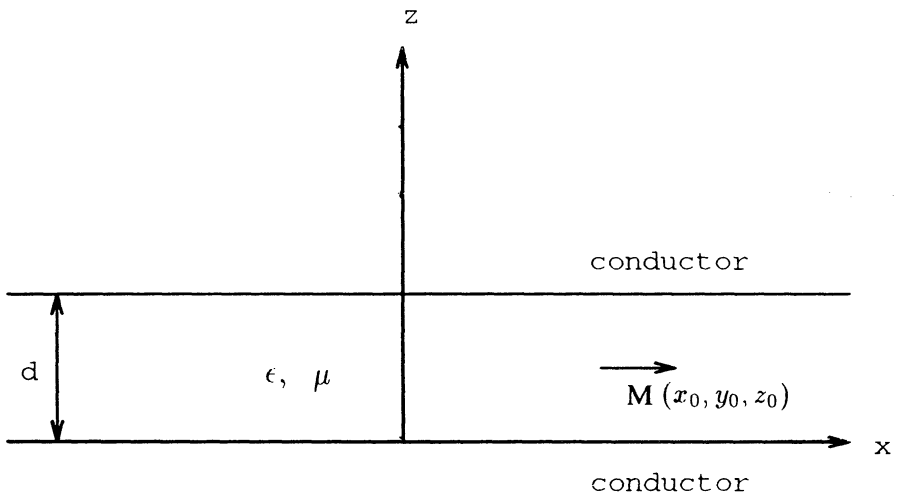

Figure 4: The structure of a two-plate waveguide.

Following shows as an example the derivation of dyadic Green's functions for a magnetic source in a two-plate waveguide using spectrum domain analysis. This method can also be applied to electric sources and other planar structure. For example, single or multilayered dielectric slabs with or without a ground plane.

As shown in Fig. 4, a magnetic current is located at (x_0, y_0, z_0) in a two-plate waveguide with separation d and permittivity ϵ, permeability μ. The vector potential, electric field, magnetic field and the source satisfy the following equations.

$$\nabla^2 \bar{F} + k^2 \bar{F} = -\epsilon \bar{M} \tag{45}$$

$$\epsilon \bar{E} = -\nabla \times \bar{F} \tag{46}$$

$$\bar{H} = -j\omega \bar{F} - \frac{j\omega}{k^2} \nabla \nabla \cdot \bar{F} \tag{47}$$

where $k^2 = \omega^2 \epsilon \mu$. Let $\bar{M} = \hat{x}\delta(x - x_0)\delta(y - y_0)\delta(z - z_0)$ be a x-directed magnetic current source. Since the magnetic source is only x-directed, it is suffice to assume that the vector potential $\bar{F} = \hat{x}F_x$. Equation (45) becomes

$$\bigtriangledown^2 F_x + k^2 F_x = -\epsilon\delta(x - x_0)\delta(y - y_0)\delta(z - z_0) \tag{48}$$

and equation (46) becomes

$$\begin{aligned} \epsilon\bar{E} &= -\begin{vmatrix} \hat{x} & \hat{y} & \hat{z} \\ \frac{\partial}{\partial x} & \frac{\partial}{\partial y} & \frac{\partial}{\partial y} \\ F_x & 0 & 0 \end{vmatrix} \\ &= -\hat{y}\frac{\partial F_x}{\partial z} + \hat{z}\frac{\partial F_x}{\partial y} \end{aligned} \tag{49}$$

Since the tangential E fields must vanish on the plates, from equation (49), F_x satisfies

$$\frac{\partial F_x}{\partial z} = 0 \qquad \text{at} \qquad z = 0, d \tag{50}$$

Assume

$$F_x = \iint G_x(k_x, k_y, z)e^{jk_x x}e^{jk_y y}dk_x dk_y, \tag{51}$$

then

$$G_x = \frac{1}{4\pi^2}\iint F_x e^{-jk_x x}e^{-jk_y y}dxdy. \tag{52}$$

Substitute equation (51) to (48), we get

$$\frac{\partial^2 F_x}{\partial z^2} + (k^2 - k_x^2 - k_y^2)F_x = -\epsilon\delta(x - x_0)\delta(y - y_0)\delta(z - z_0) \tag{53}$$

Inversely transform equation (53), we get

$$\frac{\partial^2 G_x}{\partial z^2} + (k^2 - k_x^2 - k_y^2)G_x = -\frac{\epsilon}{4\pi^2}e^{-jk_x x_0}e^{-jk_y y_0}\delta(z - z_0) \tag{54}$$

Let

$$G_x = \begin{cases} C_1 \cos k_z(z - d), & \text{for} \quad z \geq z_0 \\ C_2 \cos k_z z, & \text{for} \quad z \leq z_0 \end{cases}, \tag{55}$$

where k_z satisfies $k^2 = k_x^2 + k_y^2 + k_z^2$ and C_1, C_2 are constants to be determined. then G_x satisfies the boundary condition at $z = 0, d$. Integrate equation (54) form z_0^- to z_0^+, we get

$$\frac{\partial G_x}{\partial z}\Big]_{z_0^-}^{z_0^+} = -\frac{\epsilon}{4\pi^2} e^{-jk_x x_0} e^{-jk_y y_0} \tag{56}$$

This leads to

$$-k_z C_1 \sin k_z(z_0 - d) + k_z C_2 \sin k_z z_0 = -\frac{\epsilon}{4\pi^2} e^{-jk_x x_0} e^{-jk_y y_0} \tag{57}$$

Also G_x must continue at $z = z_0$. This leads to

$$C_1 \cos k_z(z_0 - d) = C_2 \cos k_z z_0 \tag{58}$$

From equation (57) and (58), C_1 and C_2 are solved.

$$C_1 = -\frac{\cos k_z z_0}{k_z \sin k_z d} \frac{\epsilon}{4\pi^2} e^{-jk_x x_0} e^{-jk_y y_0} \tag{59}$$

$$C_2 = -\frac{\cos k_z(z_0 - d)}{k_z \sin k_z d} \frac{\epsilon}{4\pi^2} e^{-jk_x x_0} e^{-jk_y y_0}, \tag{60}$$

and E fields and H fields can be derived from equation (45) and (46).

The above formulation gives a general procedure for deriving spectral domain Green's functions. The cases for electric sources and sources in other directions is similar.

B Green's Functions

The spectral domain kernels that are used for the Green's functions of the analysis are presented below. The following definitions are used in the expressions:

$$k_0^2 = \omega^2 \mu_0 \epsilon_0 \tag{61}$$

$$k_{1a} = (\epsilon_r^a k_0^2 - \beta^2)^{1/2}, \qquad Im\{k_{1a}\} < 0, Re\{k_{1a}\} > 0 \tag{62}$$

$$k_{1b} = (\epsilon_r^b k_0^2 - \beta^2)^{1/2}, \qquad Im\{k_{1b}\} < 0, Re\{k_{1b}\} > 0 \tag{63}$$

$$k_2 = (k_0^2 - \beta^2)^{1/2}, \qquad Im\{k_2\} < 0, Re\{k_2\} > 0 \tag{64}$$

$$\beta^2 = k_x^2 + k_y^2 \tag{65}$$

$$T_e^b = k_{1b}\cos(k_{1b}d_b) + jk_2\sin(k_{1b}d_b) \tag{66}$$

$$T_m^b = \epsilon_r^b k_2\cos(k_{1b}d_b) + jk_{1b}\sin(k_{1b}d_b) \tag{67}$$

$$Z_0 = (\mu_0/\epsilon_0)^{1/2} \tag{68}$$

The required kernel functions are

for $G^b_{EJyy}(x, y, d_b|x_0, y_0, d_b)$:

$$\begin{aligned} Q^b_{EJyy}(k_x, k_y) &= -j\frac{Z_0}{4\pi^2 k_0} \\ &\cdot\frac{(\epsilon_r^b k_0^2 - k_y^2)k_2\cos(k_{1b}d_b) + j(k_0^2 - k_y^2)k_{1b}\sin(k_{1b}d_b)}{T_e^b T_m^b} \\ &\times\sin(k_{1b}d_b) \end{aligned} \tag{69}$$

for $G^b_{HJxy}(x, y, 0|x_0, y_0, d_b)$:

$$Q^b_{HJxy}(k_x, k_y) = \frac{1}{4\pi^2}\cdot\frac{-\epsilon_r^b k_{1b}k_2\cos(k_{1b}d_b) + j(k_y^2(\epsilon_r^b - 1) - k_{1b}^2)\sin(k_{1b}d_b)}{T_e^b T_m^b} \tag{70}$$

for $G^b_{HMxx}(x, y, 0|x_0, y_0, 0)$:

$$\begin{aligned} Q^b_{HMxx}(k_x, k_y) &= \frac{-j}{4\pi^2 k_0 Z_0}\frac{1}{k_{1b}T_e^b T_m^b}\cdot[jk_x^2 k_{1b}^2(\epsilon_r^b - 1) + (\epsilon_r^b k_0^2 - k_x^2) \\ &\times\{k_{1b}k_2(\epsilon_r^b + 1)\sin(k_{1b}d_b)\cos(k_{1b}d_b) \\ &+ j(\epsilon_r^b k_2^2\sin^2(k_{1b}d_b) - k_{1b}^2\cos^2(k_{1b}d_b))\}] \end{aligned} \tag{71}$$

for $G^b_{EMyx}(x, y, d_b|x_0, y_0, 0)$

$$Q^b_{EMyx}(k_x, k_y)(k_x, k_y) = -Q^b_{HJxy}(k_x, k_y) \tag{72}$$

for $G^a_{EJyy}(x, y, z_0|x_0, y_0, z_0)$:

$$Q^a_{EJyy}(k_x, k_y) = \frac{j\omega\mu_0}{4\pi^2\epsilon_r^a k_0^2}\cdot(\epsilon_r^a k_0^2 - \beta^2)\cdot\frac{\sin k_{1a}(z_0 - d_a)\sin(k_{1a}z_0)}{k_{1a}\sin k_{1a}d_a} \tag{73}$$

for $G^a_{HJxy}(x, y, 0|x_0, y_0, z_0)$:

$$Q^a_{HJxy}(k_x, k_y) = \frac{1}{4\pi^2}\cdot\frac{\sin k_{1a}(z_0 - d_a)}{\sin(k_{1a}d_a)} \tag{74}$$

for $G^a_{HMxx}(x, y, 0|x_0, y_0, z_0)$:

$$Q^a_{HMxx}(k_x, k_y) = \frac{j\omega\epsilon^a_r}{4\pi^2} \cdot (\epsilon^a_r k_0^2 - k_y^2) \cdot \frac{\cos(k_{1a}d_a)}{k_{1a}\sin(k_{1a}d_a)} \tag{75}$$

for $G^a_{EMyx}(x, y, d_a|x_0, y_0, 0)$:

$$Q^a_{EMyx}(k_x, k_y) = -Q^a_{HJxy}(k_x, k_y) \tag{76}$$

References

[1] P.L. Sullivan and D.H. Schaubert, "Analysis of an Aperture Coupled Microstrip Antenna," *IEEE Trans. Antennas Propagat.,* vol. AP-34, pp. 977–984, Aug. 1986.

[2] D. M. Pozar, "Input impedance and mutual coupling of rectangular microstrip antennas," *IEEE Trans. Antennas Propagat.,* vol. AP-30, pp. 1191-1196, Nov. 1982.

[3] N.K. Das and D.M. Pozar, "Multiport Scattering Analysis of General Multilayered Printed Antennas Fed by Multiple Feed Ports: Part I — Theory," *IEEE Trans. Antennas Progagat.,* vol. AP-40, pp. 469–481, May 1992.

[4] N.K. Das and D.M. Pozar, "Multiport Scattering Analysis of General Multilayered Printed Antennas Fed by Multiple Feed Ports: Part II — Applications," *IEEE Trans. Antennas Progagat.,* vol. AP-40, pp. 482–490, May 1992.

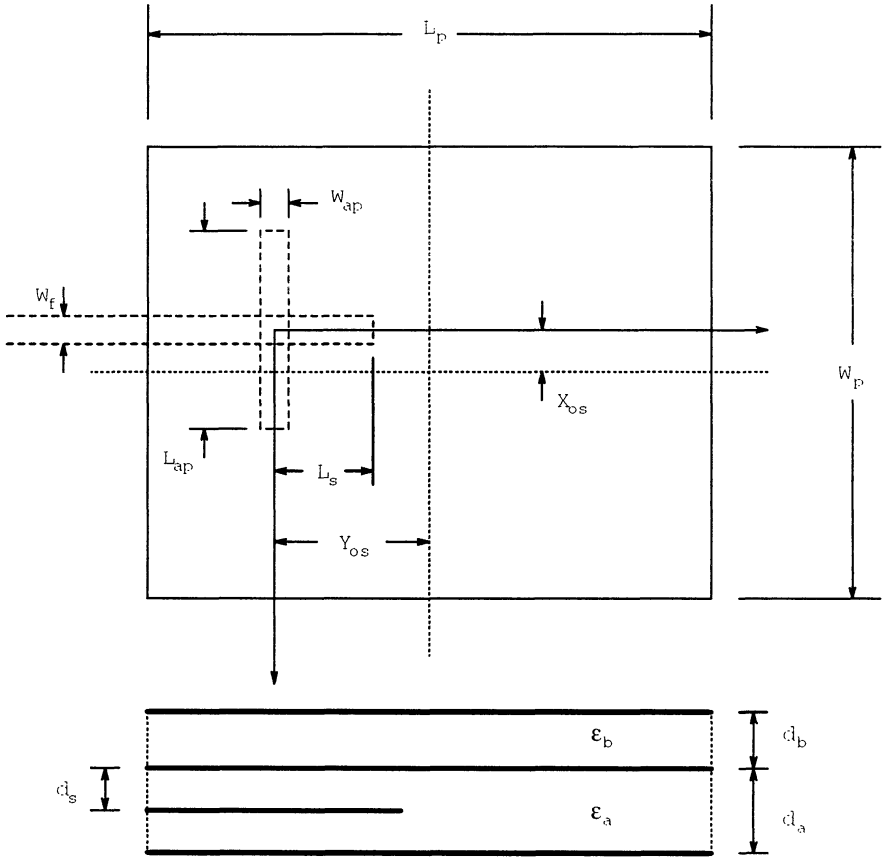

Figure 5: The notation of the parameters

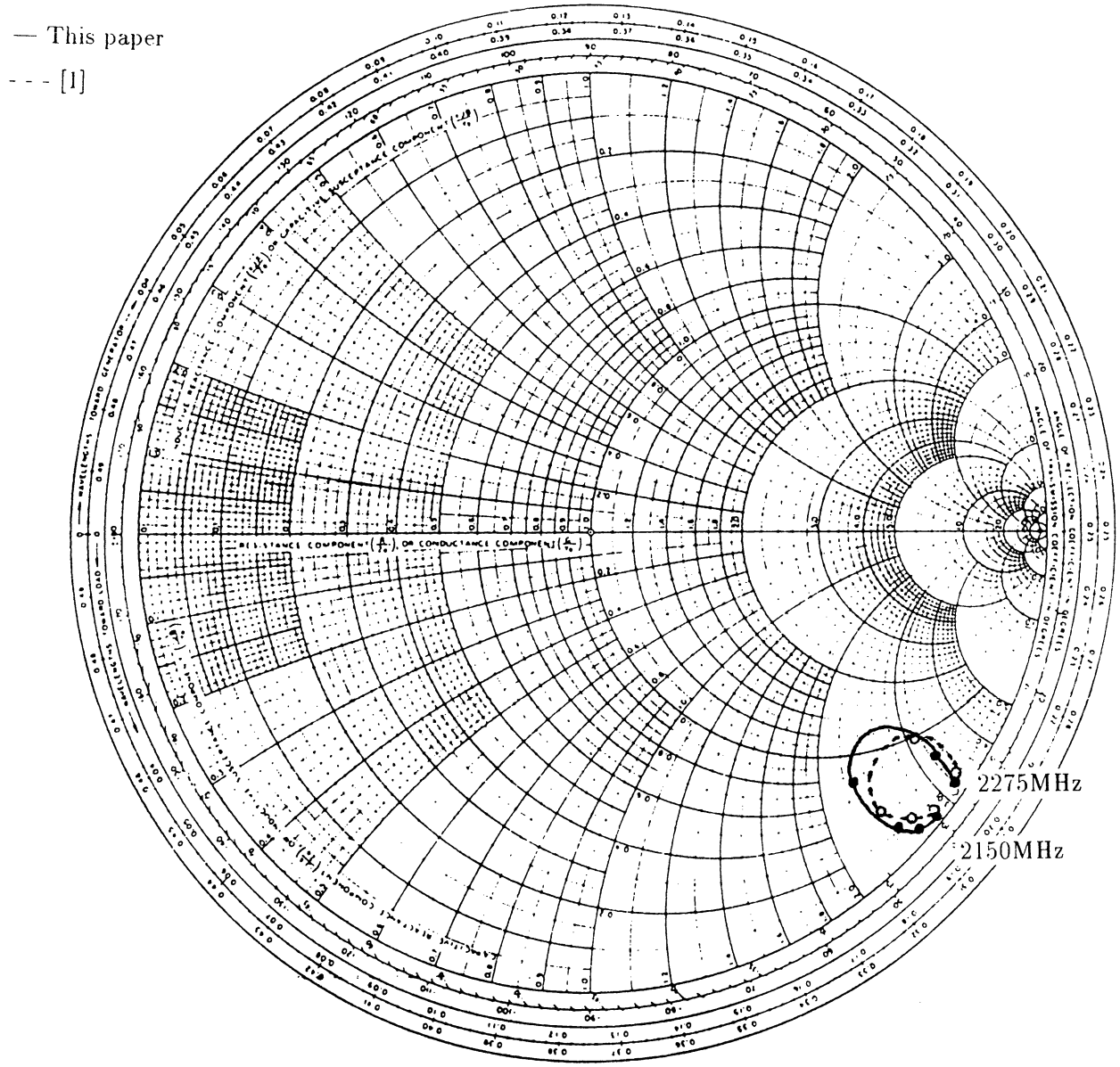

Figure 6: The calculated input impedance as a function of frequency from 2150MHz to 2275MHz with increment 25MHz. The stub length is 0.4cm. The solid line is the calculated result of this paper. The dash line is the calculated result of [1] with microstrip line feed. Note the feeding structures are different. $\epsilon_r^b = 2.54$, $d_b = 0.16$cm, $L_p = 4.0$cm, $W_p = 3.0$cm, $X_{os} = 0.0$cm, $Y_{os} = 0.0$cm, $L_{ap} = 1.12$cm, $W_{ap} = 0.155$cm, $\epsilon_r^a = 2.54$, $d_a = 0.16$cm, $W_f = 0.442$cm, $d_s = 0.08$cm.

— This paper
- - - [1]

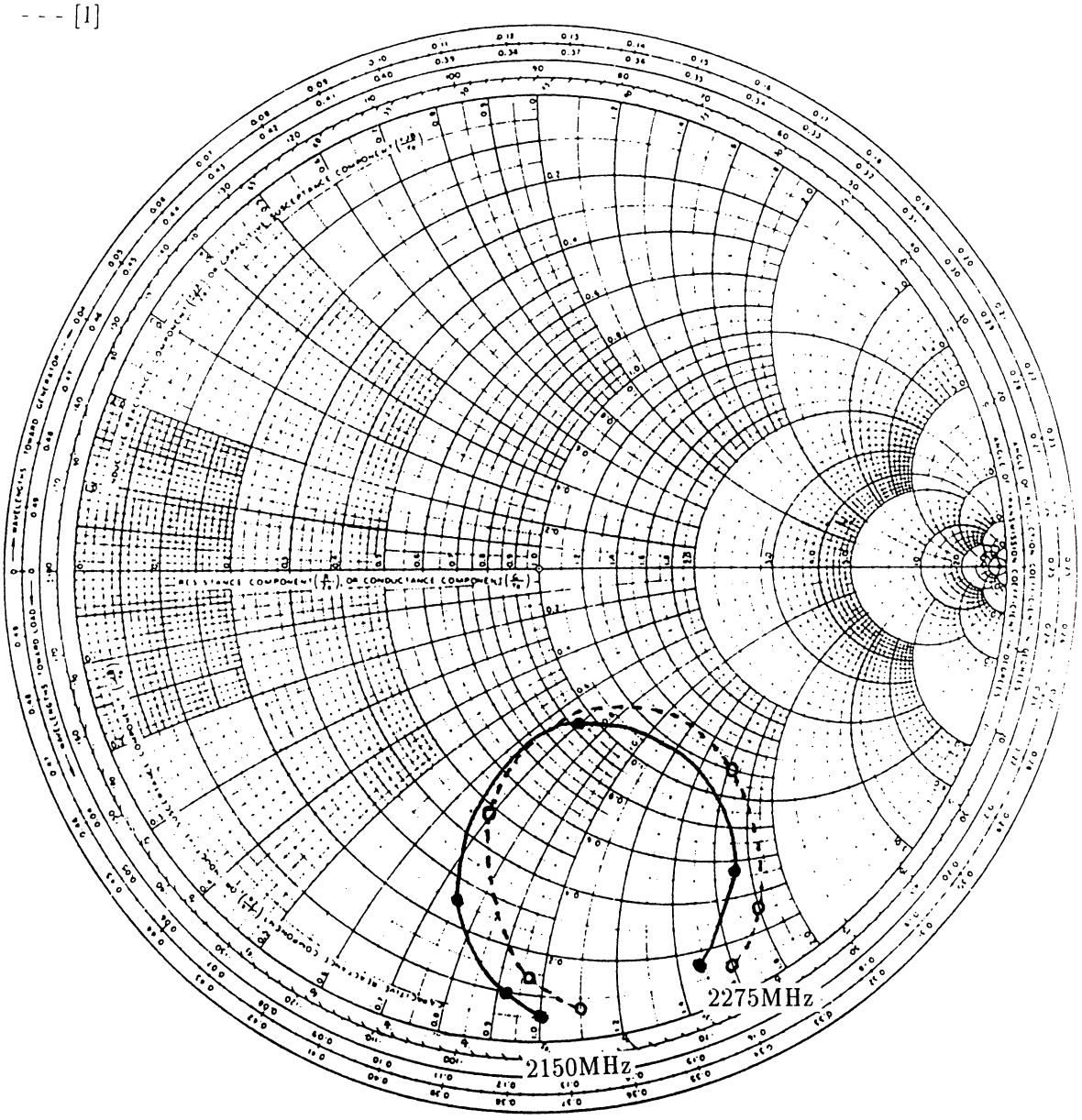

Figure 7: Same as Fig. 6 except the stub length is 0.8cm.

— This paper

- - - [1]

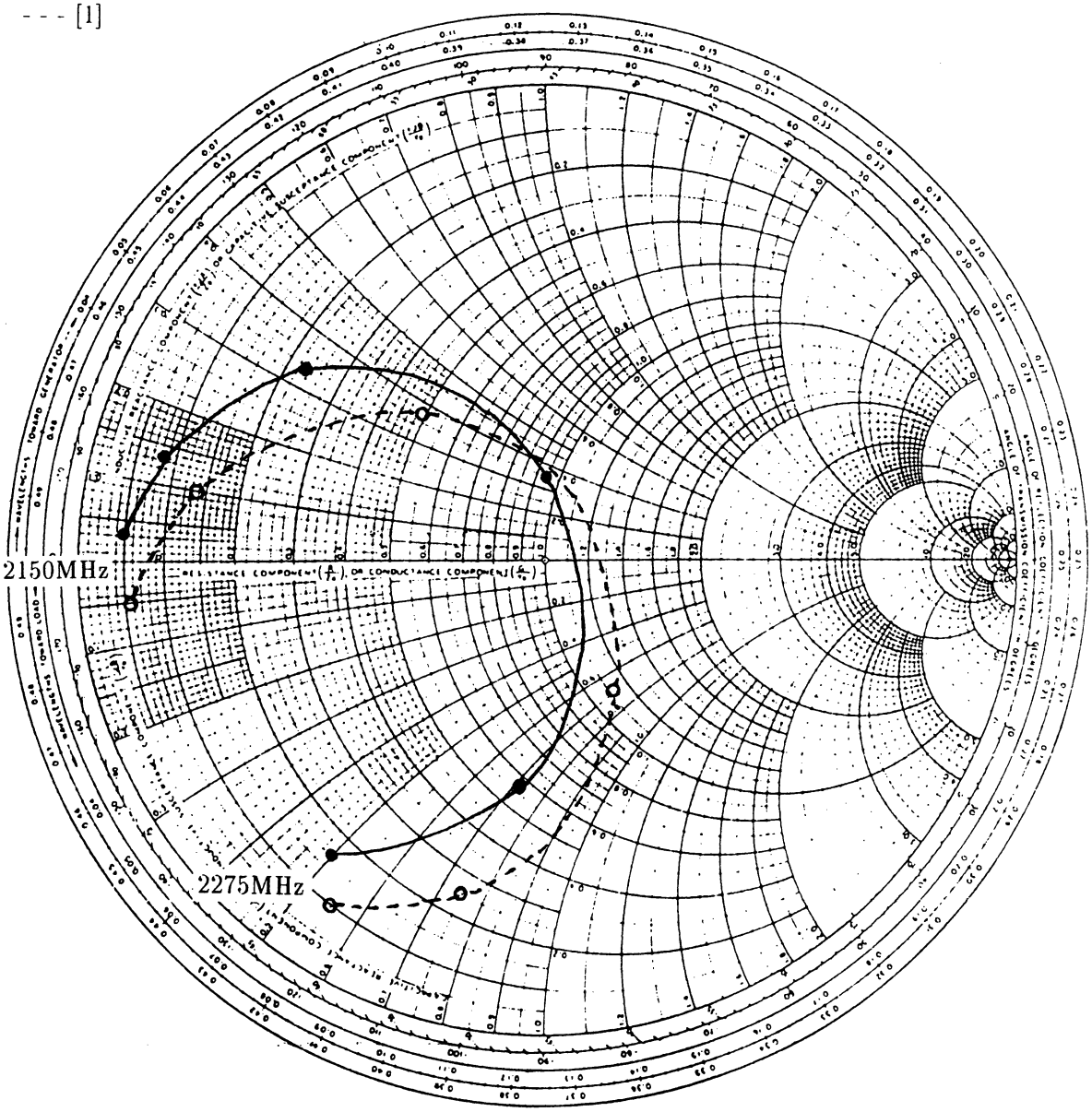

Figure 8: Same as Fig. 6 except the stub length is 1.6cm.

— This paper

- - - [1]

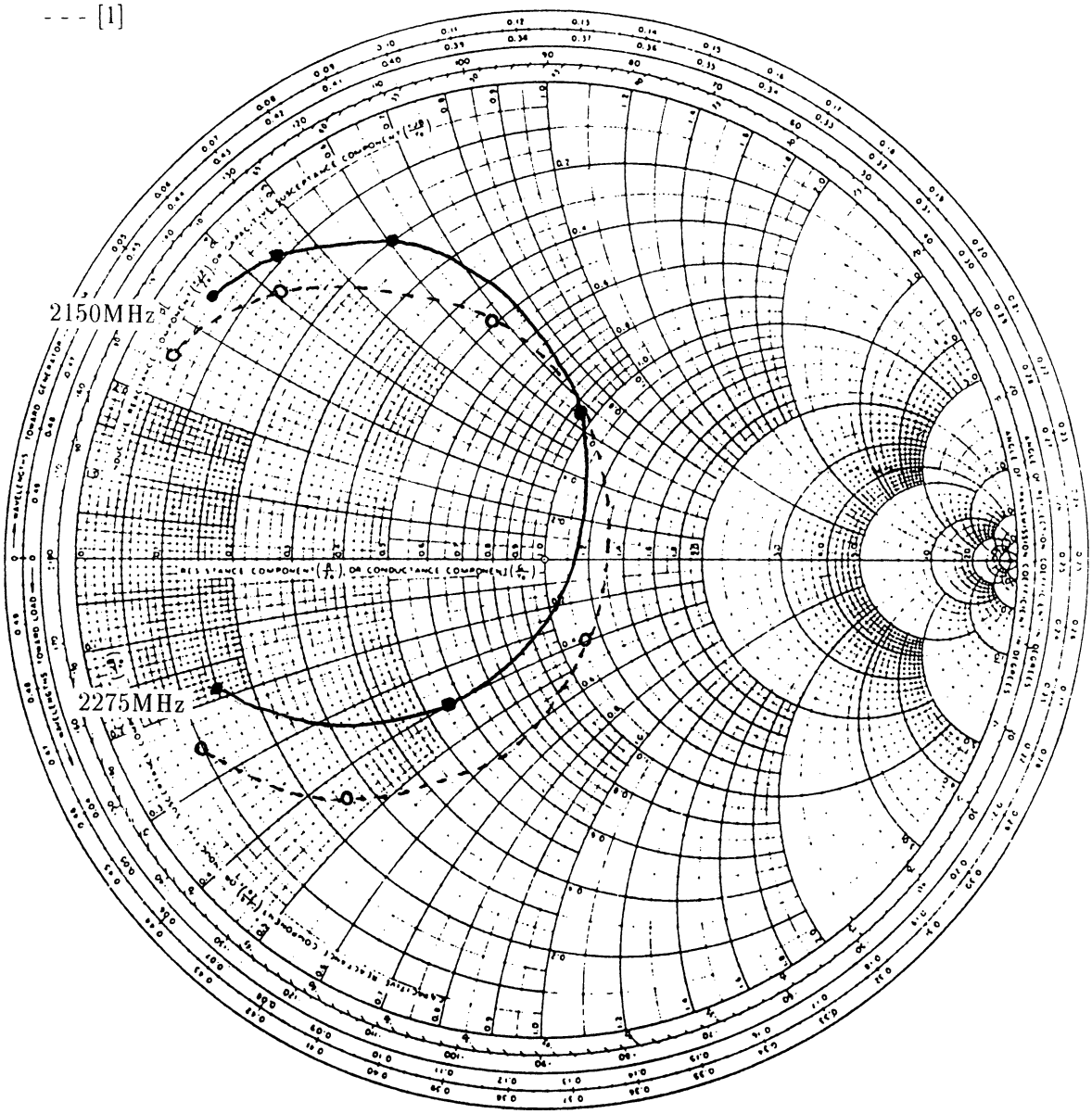

Figure 9: Same as Fig. 6 except the stub length is 2.0cm.

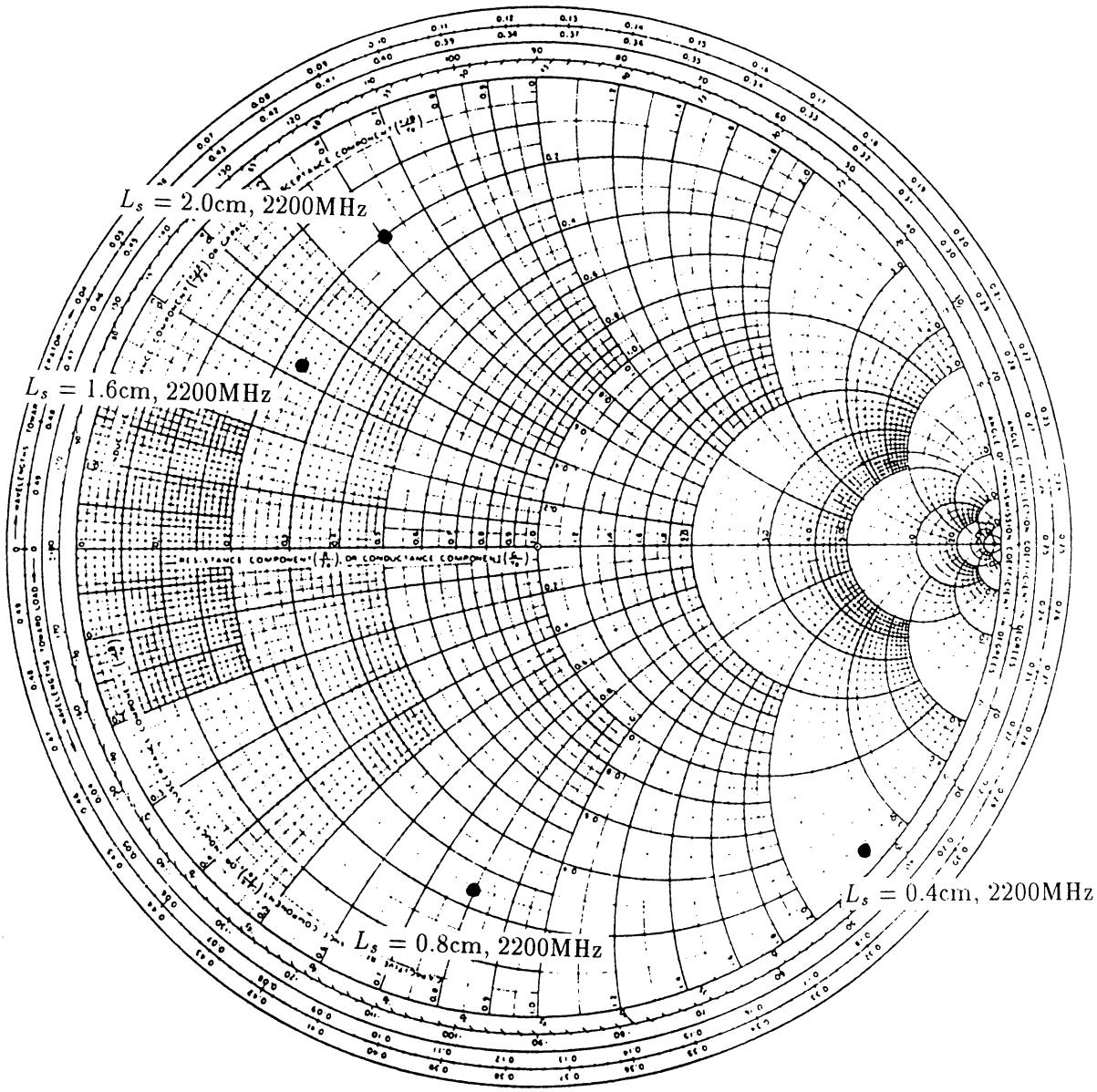

Figure 10: Input impedance as a function of stub length. Other parameters are the same as Fig. 6.